

# Generating MCMC proposals by randomly rotating the regular simplex

Andrew J. Holbrook

UCLA Biostatistics

## Abstract

We present the *simplicial sampler*, a class of parallel MCMC methods that generate and choose from multiple proposals at each iteration. The algorithm’s multiproposal randomly rotates a simplex connected to the current Markov chain state in a way that inherently preserves symmetry between proposals. As a result, the simplicial sampler does not require a proposal density term correction within its accept-reject step. It simply chooses from among the simplex nodes with probability proportional to their target density values. While the algorithm enjoys natural parallelizability, we show that conventional implementations are sufficient to confer efficiency gains across an array of dimensions and a number of target distributions.

## 1 Introduction

The majority of reversible MCMC samplers work by generating a single proposal state and using the Metropolis-Hastings criterion (Metropolis et al., 1953; Hastings, 1970) to accept or reject that proposal. Sometimes the acceptance probability is unity (Smith and Roberts, 1993), and sometimes one must account for deterministic proposal mechanisms (Green, 1995). Other times, the acceptance criterion takes on a different (but related) form (Barker, 1965; Zanella, 2020). This line of samplers has culminated in Hamiltonian Monte Carlo (Duane et al., 1987; Neal, 2011), an MCMC algorithm that scales Bayesian inference to models of unprecedented dimensionality. Despite this success, the sequential natures of many MCMC samplers result in the under-utilization of modern computational hardware designed for parallel processing. Indeed, full utilization of computational resources often requires model specific and time intensive parallelization of algorithmic bottlenecks such as the model log-likelihood or its gradient (Holbrook et al., 2021b, 2020, 2021a).

On the other hand, the seminal works of Neal (2003a), Tjelmeland (2004) and Frenkel (2004) kicked off research into a new line of MCMC methods that use multiple proposals in each MCMC step. These methods either accept a single proposal from the many or create a weighted estimator that borrows from each (Delmas and Jourdain, 2009; Calderhead, 2014; Yang et al., 2018; Schwedes and Calderhead, 2021). One may interpret these *parallel MCMC* algorithms both as simulating from a finite state Markov chain that has the different

proposals as states (Calderhead, 2014) and as a special case of the more general particle Gibbs sampler (Andrieu et al., 2010; Schwedes, 2019). As opposed to traditional MCMC methods that use a binary accept-reject step, these generally allow for greater parallelization, both in target evaluations and in proposal generations.

Within the framework established in Tjelmeland (2004), we propose a basic algorithm, the simplicial sampler, that works differently from the Metropolis-Hastings line. This algorithm proposes multiple states at each iteration and randomly selects the next Markov chain state from among these proposals in a single step. Its novel, intrinsically reversible proposal mechanism facilitates a simpler overall algorithmic structure. At the same time, the algorithm enjoys the benefits documented by its parallel MCMC predecessors: (1) its core computations are highly parallelizable; and (2) increased proposal counts generally accord with greater sampling efficiency per iteration (Calderhead, 2014). Here, we focus on the latter and demonstrate that even sequential implementations achieve significant speedups over competitors.

## 2 Basic algorithm

We wish to sample from the target distribution with density  $\pi(\boldsymbol{\theta})$  for  $\boldsymbol{\theta} \in \mathbb{R}^D$ . Given the current Markov chain state  $\boldsymbol{\theta}^{(s)}$ , we use the following steps to advance the Markov chain.

1. Propose states  $\boldsymbol{\Theta}^* = (\boldsymbol{\theta}_1^*, \dots, \boldsymbol{\theta}_P^*, \boldsymbol{\theta}_{P+1}^*) = (\boldsymbol{\theta}_1^*, \dots, \boldsymbol{\theta}_P^*, \boldsymbol{\theta}^{(s)})$  according to the distribution  $q(\boldsymbol{\theta}^{(s)}, \boldsymbol{\Theta}^*)$ ;
2. Calculate densities  $\pi(\boldsymbol{\theta}_p^*)$  for  $p = 1, \dots, P + 1$ ;
3. Randomly select a single state  $\boldsymbol{\theta}_p^*$  from the set  $\boldsymbol{\Theta}^*$  according to the selection probabilities

$$\left( \frac{\pi(\boldsymbol{\theta}_1^*)}{\sum_{p=1}^{P+1} \pi(\boldsymbol{\theta}_p^*)}, \frac{\pi(\boldsymbol{\theta}_2^*)}{\sum_{p=1}^{P+1} \pi(\boldsymbol{\theta}_p^*)}, \dots, \frac{\pi(\boldsymbol{\theta}_{P+1}^*)}{\sum_{p=1}^{P+1} \pi(\boldsymbol{\theta}_p^*)} \right); \quad (1)$$

4. Set  $\boldsymbol{\theta}^{(s+1)} = \boldsymbol{\theta}_p^*$ .

This transition rule rarely leaves the target distribution invariant. We require a further sufficient condition to guarantee that  $\pi(\boldsymbol{\theta})$  is a stationary distribution for our Markov chain.

**Proposition 1** (Tjelmeland (2004)). *The Markov chain with the above transition rule maintains detailed balance with respect to the target distribution  $\pi(\boldsymbol{\theta})$  if  $q(\cdot, \cdot)$  satisfies*

$$q(\boldsymbol{\theta}_1^*, \boldsymbol{\Theta}^*) = \dots = q(\boldsymbol{\theta}_p^*, \boldsymbol{\Theta}^*) = \dots = q(\boldsymbol{\theta}_{P+1}^*, \boldsymbol{\Theta}^*), \quad (2)$$

*and so  $\pi(\boldsymbol{\theta})$  is a stationary distribution of the chain.*

*Proof.* For proposal state  $\boldsymbol{\theta}_p^* \in \boldsymbol{\Theta}^*$ , the following holds

$$\begin{aligned}\pi(\boldsymbol{\theta}^{(s)}) p(\boldsymbol{\theta}^{(s)}, \boldsymbol{\theta}_p^*) &= \pi(\boldsymbol{\theta}_{P+1}^*) p(\boldsymbol{\theta}_{P+1}^*, \boldsymbol{\theta}_p^*) = \frac{\pi(\boldsymbol{\theta}_{P+1}^*) q(\boldsymbol{\theta}_{P+1}^*, \boldsymbol{\Theta}^*) \pi(\boldsymbol{\theta}_p^*)}{\sum_{p=1}^{P+1} \pi(\boldsymbol{\theta}_p^*)} \\ &= \frac{\pi(\boldsymbol{\theta}_p^*) q(\boldsymbol{\theta}_p^*, \boldsymbol{\Theta}^*) \pi(\boldsymbol{\theta}_{P+1}^*)}{\sum_{p=1}^{P+1} \pi(\boldsymbol{\theta}_p^*)} \\ &= \pi(\boldsymbol{\theta}_p^*) p(\boldsymbol{\theta}_p^*, \boldsymbol{\theta}_{P+1}^*) = \pi(\boldsymbol{\theta}_p^*) p(\boldsymbol{\theta}_p^*, \boldsymbol{\theta}^{(s)})\end{aligned}$$

□

This result motivates us to invent a proposal mechanism that satisfies Equation (2).

### 3 Simplicial sampling

We develop a proposal mechanism and a few variations that satisfy the symmetry relation of Equation (2) and help our basic algorithm preserve reversibility with respect to the target  $\pi(\boldsymbol{\theta})$ . Start with the simplex identified by a set of fixed vertices  $\mathbf{v}_1, \dots, \mathbf{v}_{D+1} \in \mathbb{R}^D$  that satisfy

$$\|\mathbf{v}_d - \mathbf{v}_{d'}\|_2 = \begin{cases} \lambda & d \neq d' \\ 0 & d = d' \end{cases}$$

with  $\mathbf{v}_{D+1} = \mathbf{0}$ . Equating the number of new proposals  $P$  with the state space dimension  $D$ , the simplicial sampler generates and chooses from proposals  $\boldsymbol{\theta}_1^*, \dots, \boldsymbol{\theta}_{D+1}^*$  as follows.

1. Sample  $\mathbf{Q}$  according to the uniform Haar distribution  $\mathcal{H}(\mathcal{O}_D)$  on the  $D$ -dimensional orthogonal group  $\mathcal{O}_D$  (Stewart, 1980).
2. Rotate and translate the simplicial vertices  $(\mathbf{v}_1, \dots, \mathbf{v}_D, \mathbf{0}) \mapsto \mathbf{Q}(\mathbf{v}_1, \dots, \mathbf{v}_D, \mathbf{0}) + \boldsymbol{\theta}^{(s)} =: (\boldsymbol{\theta}_1^*, \dots, \boldsymbol{\theta}_{D+1}^*)$ .
3. Draw a single sample  $\boldsymbol{\theta}_d^*$  from  $(\boldsymbol{\theta}_1^*, \dots, \boldsymbol{\theta}_{D+1}^*)$  with probability proportional to  $\pi(\boldsymbol{\theta}_d^*)$ .
4. Set  $\boldsymbol{\theta}^{(s+1)} = \boldsymbol{\theta}_d^*$ .

In short, the simplicial sampler advances its Markov chain by randomly rotating a set of  $D$  equidistant vertices about the current state  $\boldsymbol{\theta}^{(s)}$  (Figure 1) and randomly selecting the next state from among all  $D + 1$  vertices of the resulting simplex. A modified simplicial sampler that only generates a single proposal reduces to Barker's acceptance criterion (Barker, 1965)

$$\pi(\boldsymbol{\theta}^*) / (\pi(\boldsymbol{\theta}^*) + \pi(\boldsymbol{\theta}^{(s)}))$$

with a symmetric proposal distribution. Importantly, the random rotation step satisfies the symmetry relation of Equation (2).

**Lemma 1.** *The simplicial sampler multiproposal  $q(\boldsymbol{\theta}^{(s)}, \boldsymbol{\Theta}^*)$  defined by*

$$(\mathbf{v}_1, \dots, \mathbf{v}_D, \mathbf{0}) \mapsto \mathbf{Q}(\mathbf{v}_1, \dots, \mathbf{v}_D, \mathbf{0}) + \boldsymbol{\theta}^{(s)} =: (\boldsymbol{\theta}_1^*, \dots, \boldsymbol{\theta}_{D+1}^*) \quad \text{for } \mathbf{Q} \sim \mathcal{H}(\mathcal{O}_D)$$

*satisfies the symmetry relation of Equation (2), namely*

$$q(\boldsymbol{\theta}_1^*, \boldsymbol{\Theta}^*) = \dots = q(\boldsymbol{\theta}_d^*, \boldsymbol{\Theta}^*) = \dots = q(\boldsymbol{\theta}_{D+1}^*, \boldsymbol{\Theta}^*).$$

*Proof.* Start by translating coordinates so that  $\boldsymbol{\theta}^{(s)} = \mathbf{0}$ . We want to show that  $q(\mathbf{0}, \boldsymbol{\Theta}^*) = q(\boldsymbol{\theta}_d^*, \boldsymbol{\Theta}^*)$  for an arbitrary  $\boldsymbol{\theta}_d^* \in \boldsymbol{\Theta}^*$ . We focus on the case  $d \leq D$ , since the alternative case is trivial. Since the Haar measure  $\mathcal{H}(\mathcal{O}_D)$  is uniform on  $\mathcal{O}_D$ , we only need to show the existence of a rotation  $\mathbf{Q}_d \in \mathcal{O}_D$  that maps

$$(\mathbf{v}_1, \dots, \mathbf{v}_D) \mapsto (\boldsymbol{\theta}_1^*, \dots, \boldsymbol{\theta}_{d-1}^*, \mathbf{0}, \boldsymbol{\theta}_{d+1}^*, \dots, \boldsymbol{\theta}_D^*).$$

The key is recognizing that the unique reflection  $\mathbf{R}$  that exchanges  $\mathbf{0}$  and  $\boldsymbol{\theta}_d^*$  leaves all other vertices unchanged because they are equidistant from  $\mathbf{0}$  and  $\boldsymbol{\theta}_d^*$  and inhabit the hyperplane that splits them evenly. In symbols,  $\mathbf{R}\boldsymbol{\theta}_{d'}^* = \boldsymbol{\theta}_{d'}^*$  for  $d' \neq d$ . Thus

$$\mathbf{Q}^T \mathbf{R} \boldsymbol{\theta}_{d'}^* = \mathbf{Q}^T \boldsymbol{\theta}_{d'}^* = \mathbf{v}_{d'}, \quad \forall d' \neq d,$$

and

$$\mathbf{Q}^T \mathbf{R} \mathbf{0} = \mathbf{Q}^T \boldsymbol{\theta}_d^* = \mathbf{v}_d.$$

It follows that  $(\mathbf{Q}^T \mathbf{R})^T = \mathbf{R} \mathbf{Q}$  is the desired rotation matrix  $\mathbf{Q}_d$ . □

Taken together, Lemma 1 and Proposition 1 assert that the simplicial sampler maintains detailed balance with respect to the target distribution.

**Theorem 1.** *If the simplicial sampler's multiproposal is  $\pi$ -irreducible and absolutely continuous with respect to  $\pi(\boldsymbol{\theta})$ , then  $\pi(\boldsymbol{\theta})$  is the unique stationary and limiting distribution of the Markov chain, and the strong law of large numbers holds.*

*Proof.* The result is a simple combination of the sampler's reversibility with respect to  $\pi(\boldsymbol{\theta})$  and the aperiodicity that arises from its self-loop, i.e., the ability to set  $\boldsymbol{\theta}^{(s+1)}$  to  $\boldsymbol{\theta}^{(s)}$  (Tierney, 1994). □

## 3.1 Variations

### 3.1.1 Gaussian simplicial sampling

If we scale the simplex edge lengths by the square root of a chi-square random variable, the proposals will have multivariate Gaussian marginal distributions. The orthogonal group  $\mathcal{O}_D$  acts transitively on the sphere  $\mathcal{S}^{D-1}$ , i.e., it takes any point on  $\mathcal{S}^{D-1}$  to any other (Lee, 2012). For this reason, left multiplying a single point on  $\mathcal{S}^{D-1}$  by a Haar distributed rotation matrix  $\mathbf{Q} \sim \mathcal{H}(\mathcal{O}_D)$  is one method for drawing a sample from the sphere's uniform

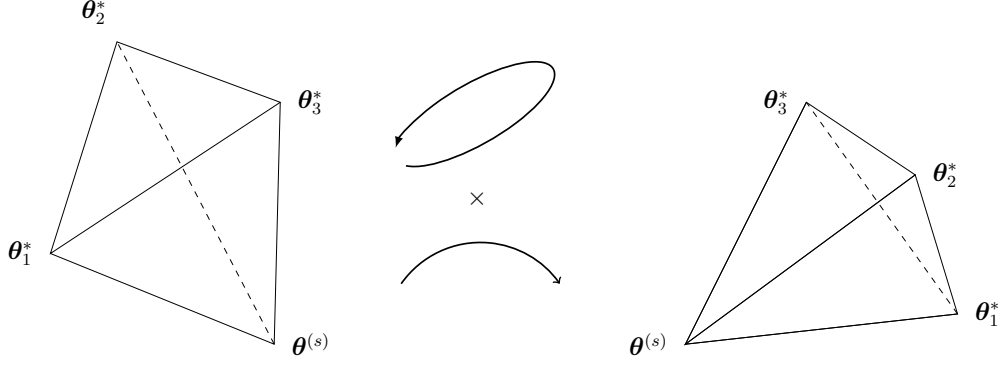


Figure 1: A simplicial sampling multiproposal

distribution. On the other hand, it is a well known fact that one may obtain a standard  $D$ -dimensional Gaussian vector by uniformly sampling a single point on the sphere  $\mathcal{S}^{D-1}$  and scaling that point by the square root of an independently sampled  $\chi^2$  random variable with  $D$  degrees of freedom. Randomly scaling the simplicial edge length in a similar manner provides the following variation that we call the *Gaussian simplicial sampler*.

1. Independently sample  $r \sim \chi^2(D)$  and  $\mathbf{Q} \sim \mathcal{H}(\mathcal{O}_D)$ .
2. Rotate, scale and translate the vertices  $(\mathbf{v}_1, \dots, \mathbf{v}_D, \mathbf{0}) \mapsto \sqrt{r}\mathbf{Q}(\mathbf{v}_1, \dots, \mathbf{v}_D, \mathbf{0}) + \boldsymbol{\theta}^{(s)} =: (\boldsymbol{\theta}_1^*, \dots, \boldsymbol{\theta}_{D+1}^*)$ .
3. Draw a single sample  $\boldsymbol{\theta}_d^*$  from  $(\boldsymbol{\theta}_1^*, \dots, \boldsymbol{\theta}_{D+1}^*)$  with probability proportional to  $\pi(\boldsymbol{\theta}_d^*)$ .
4. Set  $\boldsymbol{\theta}^{(s+1)} = \boldsymbol{\theta}_d^*$ .

By the above discussion, each of the proposals  $\boldsymbol{\theta}_d^*$  for  $d = 1, \dots, D$  has a Gaussian marginal distribution with mean  $\boldsymbol{\theta}^{(s)}$  and covariance matrix  $\lambda^2 \mathbf{I}_D$ , where  $\lambda$  is still the simplicial edge length. Because of its random scaling, a stronger result than Theorem 1 applies to the Gaussian simplicial sampler.

**Corollary 1** (of Theorem 1). *Any distribution  $\pi(\boldsymbol{\theta})$  with support  $\mathbb{R}^D$  is the unique stationary and limiting distribution of the Gaussian simplicial sampler that targets it, and the strong law of large numbers holds.*

*Proof.* All that needs to be established is  $\pi$ -irreducibility and absolute continuity. The former is accomplished by the sufficient condition (Tierney, 1994) that

$$\int_A q(\boldsymbol{\theta}_0, \boldsymbol{\Theta}^*) d\boldsymbol{\theta}_d^* > 0, \quad \text{if} \quad \int_A \pi(\boldsymbol{\theta}) d\boldsymbol{\theta} > 0, \quad d = 1, \dots, D, \quad A \subset \mathbb{R}^D.$$

This condition is itself accomplished by the unbounded nature of the multiproposal's  $\chi^2$  scaling. The latter is accomplished by hypothesis.  $\square$

In Section 4, we show that its random scaling gives the Gaussian simplicial sampler improved performance for a multimodal target distribution.

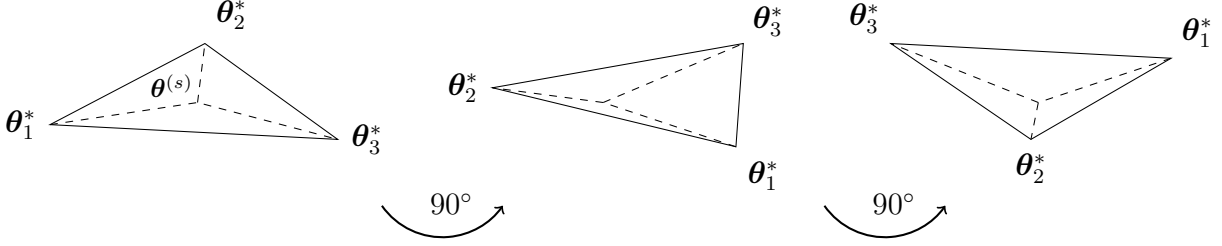


Figure 2: Rotations with respect to a non-standard Euclidean metric

### 3.1.2 Preconditioned simplicial sampling

For  $\mathbf{C} \succ \mathbf{0}$ , a  $D \times D$  and real-valued matrix, the *preconditioned simplicial sampler* takes the following steps.

1. Sample  $\mathbf{Q} \sim \mathcal{H}(\mathcal{O}_D)$ .
2. Rotate, precondition and translate the vertices  $(\mathbf{v}_1, \dots, \mathbf{v}_D, \mathbf{0}) \mapsto \mathbf{C}^{1/2}\mathbf{Q}(\mathbf{v}_1, \dots, \mathbf{v}_D, \mathbf{0}) + \boldsymbol{\theta}^{(s)} =: (\boldsymbol{\theta}_1^*, \dots, \boldsymbol{\theta}_{D+1}^*)$ .
3. Draw a single sample  $\boldsymbol{\theta}_d^*$  from  $(\boldsymbol{\theta}_1^*, \dots, \boldsymbol{\theta}_{D+1}^*)$  with probability proportional to  $\pi(\boldsymbol{\theta}_d^*)$ .
4. Set  $\boldsymbol{\theta}^{(s+1)} = \boldsymbol{\theta}_d^*$ .

The matrix  $\mathbf{C}^{1/2}\mathbf{Q}$  is itself a rotation in the Euclidean space equipped with inner product  $\langle \mathbf{v}, \mathbf{v}' \rangle_{\mathbf{C}^{-1}} := \mathbf{v}^T \mathbf{C}^{-1} \mathbf{v}'$  (Figure 2).

**Corollary 2** (of Theorem 1). *The guarantees of Theorem 1 apply to the preconditioned simplicial sampler as well.*

*Proof.* The preconditioned simplicial sampler maintains detailed balance with respect to its target distribution  $\pi(\boldsymbol{\theta})$  because it satisfies the symmetry relation of Equation (2). The proof takes the exact same form as that of Lemma 1, replacing  $\mathbf{Q}_d$  with  $\mathbf{C}^{1/2}\mathbf{Q}_d$ .  $\square$

### 3.1.3 Adaptive simplicial sampling

As has been established for other MCMC algorithms, it is often useful to adapt the simplicial sampler multiproposal. We employ two distinct methods of adaptation in Section 4. Both methods use the diminishing adaptation strategy (Rosenthal, 2011), which sacrifices guarantees of a strong law of large numbers but maintains a weak law. The first adapts all simplex edge lengths while keeping them equal so as to achieve a desired ‘acceptance’ rate. Although the simplicial sampler does not use a classical accept-reject step, we can check whether state  $\boldsymbol{\theta}^{(s+1)}$  equals  $\boldsymbol{\theta}^{(s)}$  and call this an acceptance or rejection accordingly. The second adapts the preconditioning matrix  $\mathbf{C}$  following the proposal covariance adaptation outlined in Haario et al. (2001). In practice, we find it useful to combine these two adaptation schemes when implementing the preconditioned simplicial sampler.

### 3.1.4 Extra-dimensional simplicial sampling

The final variation for the simplicial sampler uses a number of proposals that is larger than the dimensionality of the target distribution, i.e.,  $P > D$ . Let  $\mathbf{W} = [\mathbf{I}_{D \times D}, \mathbf{0}_{D \times (P-D)}]$  be the wide  $D \times P$  matrix for which multiplication selects the first  $D$  elements of any  $P$ -vector. Letting each  $\mathbf{v}_p$ ,  $p = 1, \dots, P$ , be a  $P$ -dimensional vector, the *extra-dimensional simplicial sampler* works as follows.

1. Sample  $\mathbf{Q} \sim \mathcal{H}(\mathcal{O}_P)$ .
2. Rotate, precondition and translate the vertices  $(\mathbf{v}_1, \dots, \mathbf{v}_P, \mathbf{0}) \mapsto \mathbf{Q}(\mathbf{v}_1, \dots, \mathbf{v}_P, \mathbf{0}_P) + (\boldsymbol{\theta}^{(s)T}, \mathbf{0}_{P-D}^T)^T =: (\boldsymbol{\theta}_1^*, \dots, \boldsymbol{\theta}_{P+1}^*)$ .
3. Draw a single sample  $\mathbf{W}\boldsymbol{\theta}_p^*$  from  $\mathbf{W}(\boldsymbol{\theta}_1^*, \dots, \boldsymbol{\theta}_{P+1}^*)$  with probability proportional to  $\pi(\mathbf{W}\boldsymbol{\theta}_p^*)$ .
4. Set  $\boldsymbol{\theta}^{(s+1)} = \mathbf{W}\boldsymbol{\theta}_p^*$ .

We provide no theoretical guarantees for the extra-dimensional simplicial sampler, but limited empirical experiments *do* show the algorithm providing accurate results (Section A). We visualize the sampler in Section 4.3.

## 4 Results

In the following, we use (PC-)Simpl, (PC-)RWM and (PC-)MTM to indicate the (preconditioned) simplicial sampler, random walk and multiple-try Metropolis algorithms, respectively. Although PC-RWM is better known as the adaptive Metropolis algorithm of Haario et al. (2001), we use this notation to clarify comparisons. ESS and ESSs denote effective sample size and effective sample size per second, respectively. All experiments use the R language (Ihaka and Gentleman, 1996) and the R package PRACMA (Borchers, 2021) to produce random rotations, which itself uses the QR decomposition of a matrix with Gaussian entries. Note that faster methods exist (Stewart, 1980) and would plausibly improve ESSs performance. Finally, all results herein rely on a conventional single-core implementation.

### 4.1 Empirically optimal scaling

**Acceptance rates and edge lengths** We first investigate Simpl and PC-Simpl performance for Gaussian targets of varying dimensions (4 through 500) as a function of acceptance rate and simplex edge length. For each dimension, we employ 20 independent MCMC runs of 10,000 iterations targeting one of 20 acceptance rates uniformly spaced between 0.2 and 0.95 (Section 3.1.3). The ‘ill-conditioned’ Gaussian target has diagonal covariance with elements 1 through  $D$ . The left two panels of Figure 3 plot the acceptance rates or edge lengths that maximize minimum and mean ESS out of the 20 targeted. For both Simpl and PC-Simpl, optimal acceptance rates increase with dimensionality until flattening out at around 0.675. For Simpl, optimal edge lengths quickly flatten out at around 3. For PC-Simpl, optimal edge lengths grow with target dimension.

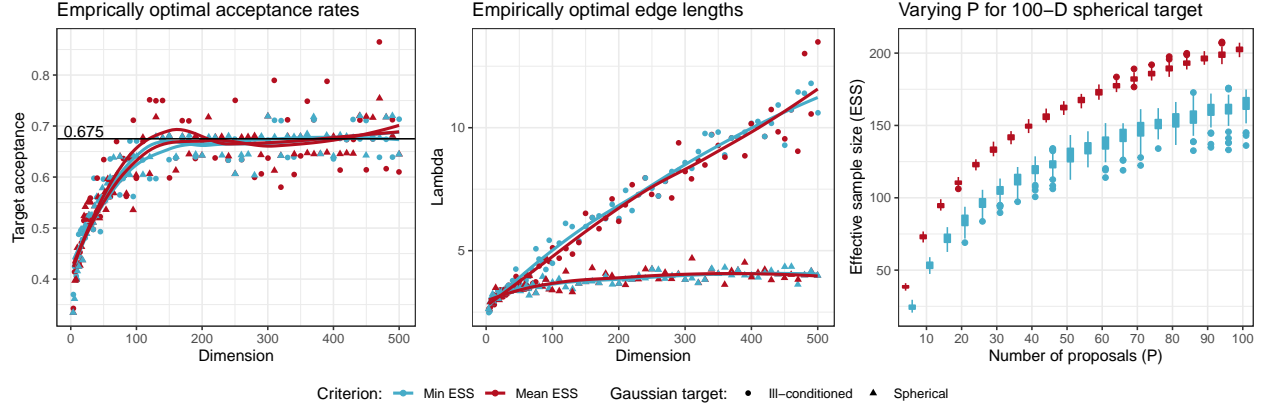


Figure 3: The left two figures present acceptance rates and simplex edge lengths that empirically maximize mean and minimum effective sample sizes (ESS) across target dimensions. For spherical and ill-conditioned targets, we use vanilla and preconditioned simplicial sampler, respectively. The right figure presents ESS results for a sampler modified to use a lower dimensional simplex.

**Number of proposals** In general, Simpl uses a simplex with  $D + 1$  nodes, the maximal number available in  $D$  dimensions. The right panel of Figure 3 shows ESS results when lower dimensional simplices (with fewer nodes) are used to generate fewer proposals ( $P < D$ ). We use 100 independent MCMC runs of 10,000 iterations each to generate minimum and mean ESS across target dimensions. Both measures improve with greater numbers of proposals. We do not compare ESSs because the additional cost of a simplex node arises from a mere  $\mathcal{O}(D^2)$  matrix-vector multiplication, compared to the  $\mathcal{O}(D^3)$  generation of a random rotation.

## 4.2 Performance comparisons

**Gaussian targets** We compare vanilla algorithms on spherical targets of dimensions  $D = 4, 8, 16, 32, 64, 128, 256$  and 512, all with identity for covariance matrix, and preconditioned algorithms on targets with ill-conditioned diagonal and full covariance matrices. Ill-conditioned matrices all have spectra ranging uniformly from 1 to  $D$ . RWM and MTM both use optimal scaling of (Gelman et al., 1997). Simpl adapts to empirically optimal acceptance rates of Figure 3. Figure 4 shows relative ESS and ESSs results from 10 independent MCMC runs of 10,000 iterations each per algorithm. Since ESS is a univariate measure, we report means and minima with respect to target dimensions.

**Bimodal target** In general, Gaussian simplicial sampling (G-Simpl) (Section 3.1.1) and its preconditioned form (PCG-Simpl) perform slightly worse (10% less ESS) than Simpl and PC-Simpl on unimodal targets, but G-Simpl and PCG-Simpl perform better on multimodal targets. We compare G-Simpl and PCG-Simpl to RWM and PC-RWM on mixture of Gaussian targets of dimensions 2, 3 and 4. Mixture probabilities are 0.5-0.5 and covariances are identity, but modal means are  $\mathbf{0}$  and  $\mathbf{5} = (5, \dots, 5)$ . Thus, modes become farther apart with increasing dimension. Figure 5 shows stacked traceplots and boxplots for the number of intermodal jumps recorded from 100 independent MCMC runs of 100,000 iterations each.



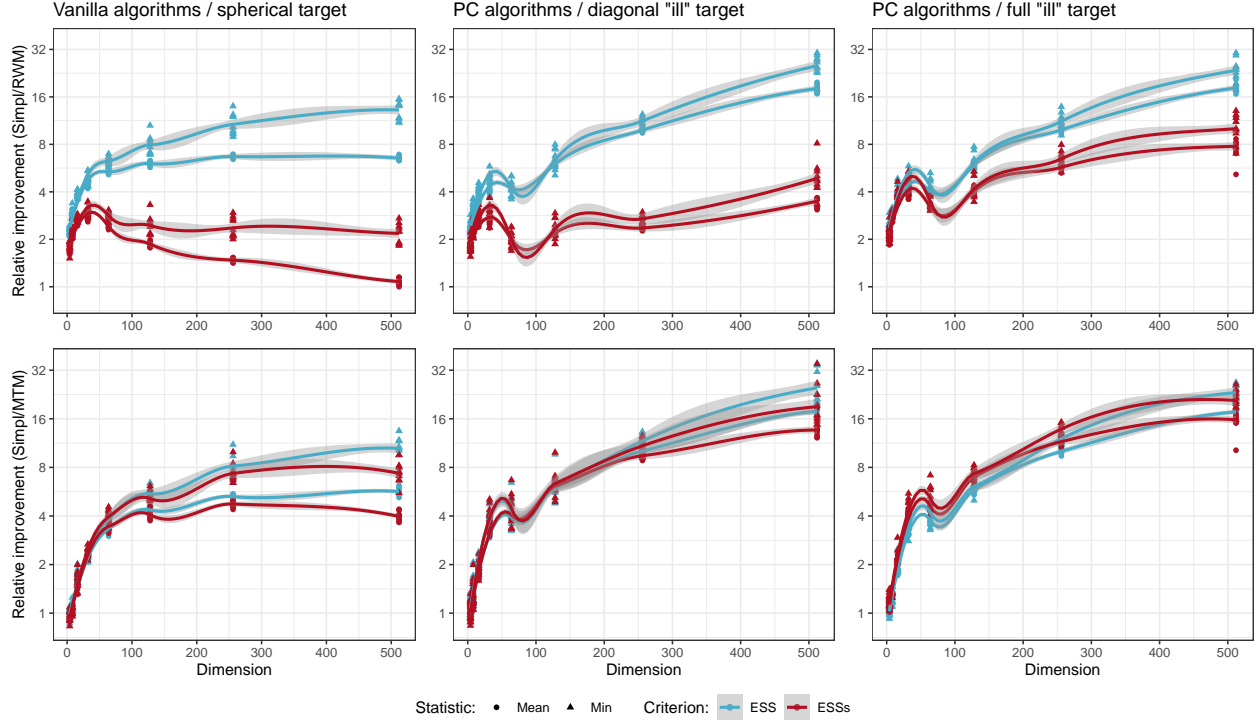


Figure 4: Relative improvement of simplicial sampler (*Simpl*) against random walk Metropolis (*RWM*) and multiple-try Metropolis (*MTM*) as measured by effective sample size (*ESS*) and *ESS* per second (*ESSs*). We apply preconditioning (*PC*) in the exact same manner to all algorithms.

Table 1: Effective sample sizes (*ESS*) and *ESS* per second (*ESSs*) from 100 independent MCMC runs of 100,000 iterations each for Gaussian process classification of 48 state election results from 2016 U.S. presidential election. Standard errors of empirical mean estimates accompany in parentheses. *Simpl*, *RWM* and *MTM* are vanilla simplicial sampler, random walk and multiple-try Metropolis algorithms. *PC* implies preconditioning. *Its* and *time to err = 10* represent iterations and seconds to achieve a misclassification total of 10, a rough measure of convergence speed. Winners in blue.

Algorithm	Mean ESS $\theta$	Min ESS $\theta$	Its to <i>err</i> = 10	ESS $\eta^2$	ESS $\xi^2$	ESS $\rho^2$	ESS $\sigma^2$
<i>Simpl</i>	1571.50 (15.6)	256.27 (6.4)	73.05 (1.8)	671.39 (10.2)	2463.76 (76.6)	3703.05 (50.0)	452.30 (6.7)
<i>RWM</i>	436.34 (2.3)	68.36 (2.3)	276.60 (8.3)	258.63 (5.7)	1407.88 (61.8)	1837.47 (31.3)	134.91 (2.3)
<i>MTM</i>	895.40 (9.2)	217.59 (6.4)	1971.21 (22.6)	604.73 (12.0)	2243.64 (83.2)	3000.50 (63.5)	316.09 (5.4)
<i>PC-Simpl</i>	1865.18 (14.4)	1200.50 (20.4)	76.39 (2.2)	1312.98 (18.0)	4583.21 (95.5)	4222.10 (50.7)	532.49 (6.5)
<i>PC-RWM</i>	362.99 (4.5)	205.16 (5.3)	284.27 (10.5)	418.99 (10.9)	1381.00 (37.6)	1654.35 (29.8)	125.12 (3.0)
<i>PC-MTM</i>	946.34 (10.3)	561.68 (12.1)	1737.98 (17.1)	825.04 (12.3)	3100.08 (92.3)	3199.16 (53.0)	263.76 (5.5)
	Mean ESSs $\theta$	Min ESSs $\theta$	Time to <i>err</i> = 10	ESSs $\eta^2$	ESSs $\xi^2$	ESSs $\rho^2$	ESSs $\sigma^2$
<i>Simpl</i>	5.62 (0.06)	0.92 (0.02)	15.87 (0.98)	2.40 (0.04)	8.81 (0.28)	13.24 (0.18)	1.62 (0.02)
<i>RWM</i>	2.50 (0.02)	0.39 (0.01)	145.41 (9.69)	1.48 (0.03)	8.09 (0.36)	10.55 (0.19)	0.77 (0.01)
<i>MTM</i>	2.88 (0.03)	0.70 (0.02)	12236.38 (294.66)	1.95 (0.04)	7.22 (0.27)	9.66 (0.21)	1.02 (0.02)
<i>PC-Simpl</i>	5.09 (0.13)	3.30 (0.10)	23.99 (1.46)	3.58 (0.10)	12.59 (0.43)	11.53 (0.32)	1.45 (0.04)
<i>PC-RWM</i>	1.44 (0.04)	0.81 (0.03)	268.77 (39.96)	1.65 (0.06)	5.48 (0.22)	6.54 (0.21)	0.49 (0.02)
<i>PC-MTM</i>	2.30 (0.06)	1.37 (0.05)	13641.57 (533.11)	2.00 (0.06)	7.58 (0.32)	7.75 (0.22)	0.64 (0.02)

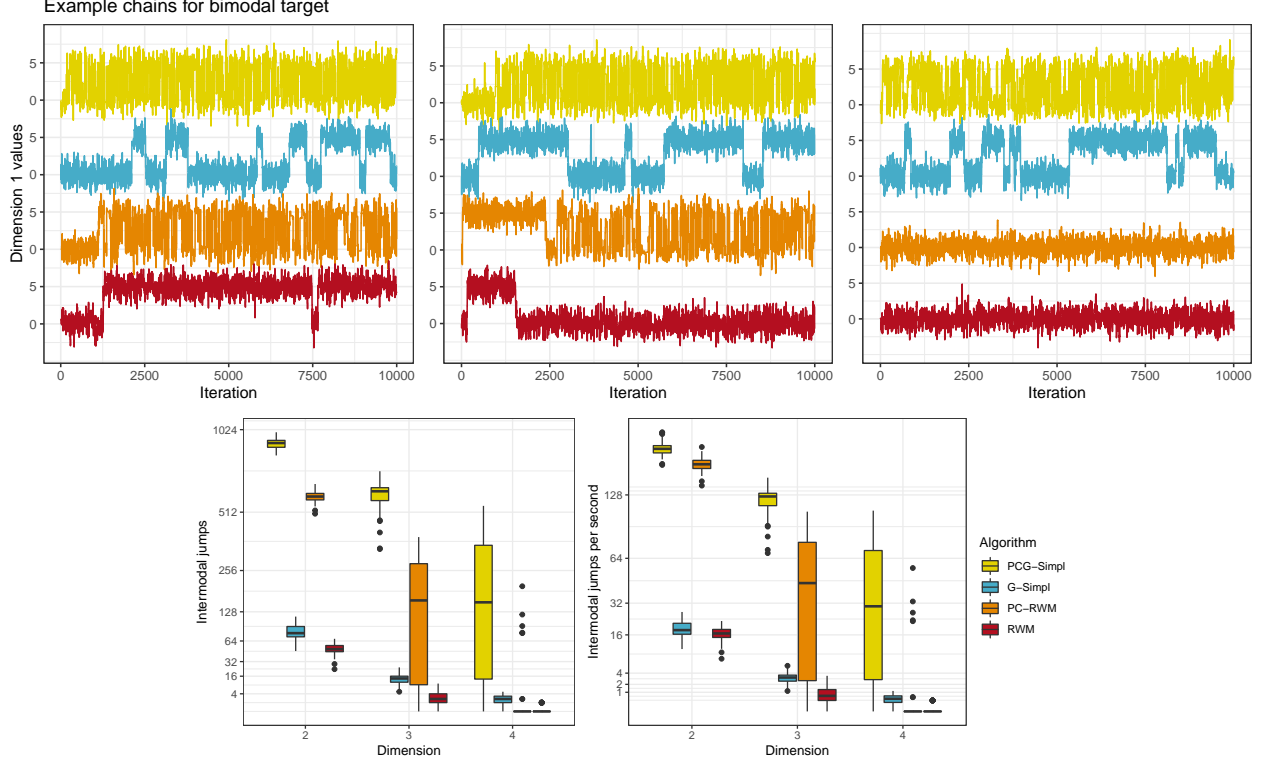


Figure 5: The top figures show stacked traceplots for the first dimension of a 3D Gaussian mixture target. The bottom figures show the number of intermodal jumps for 100,000 iterations presented over 100 independent MCMC runs. PCG- and G-Simpl are preconditioned and non-preconditioned Gaussian simplicial samplers compared to the same for random walk Metropolis (RWM).

**Gaussian process classification** 48 states use a winner-take-all rule when assigning electoral college votes during the U.S. presidential election. We use a Gaussian process (GP) with logit link (Williams and Barber, 1998) to regress binary outcomes (Trump or Clinton) over state center (latitude and longitude) and population data for the 2016 presidential election. For latent variables  $\boldsymbol{\theta} = (\theta_1, \dots, \theta_{48})$ , the prior covariance of  $\theta_i$  and  $\theta_j$  is

$$\kappa(\mathbf{x}_i, \mathbf{x}_j) = \xi^2 + \eta^2 \exp(-\rho^2 \|\mathbf{x}_i - \mathbf{x}_j\|_2^2) + \sigma^2 \delta_{ij},$$

where  $\mathbf{x}_i$  and  $\mathbf{x}_j$  are their respective predictor vectors. We infer latent variables  $\boldsymbol{\theta}$  using (PC-)Simple, (PC-)RWM and (PC-)MTM. We let Simpl algorithms target an acceptance rate of 0.5 following the results of Figure 3, while we let RWM and MTM target 0.234. We know that this acceptance target is optimal for RWM (Rosenthal, 2011) and it also appears to work well for MTM. We infer other parameters using univariate slice samplers (Neal, 2003b). Table 1 shows results from 100 independent runs of 100,000 iterations each. We initialize all chains to misclassify all states and use a total misclassification of 10 as rough convergence threshold.

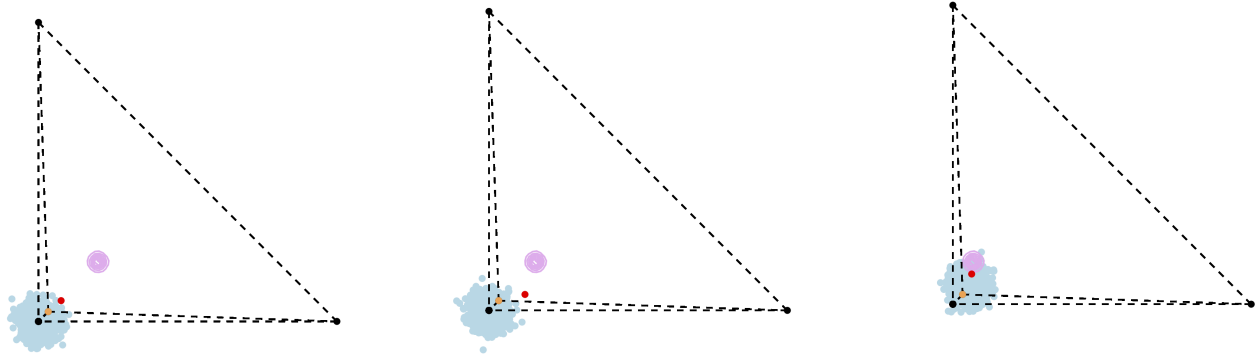


Figure 6: Successive iterations of an extra-dimensional simplicial sampler using 1000 proposals to sample a bivariate Gaussian target. For each step, the yellow dot is the initial position, the black dots are the projected un-rotated simplex vertices, the blue dots are the proposals (or projected rotated vertices), and the red dots are the accepted proposals. The dashed lines represent simplex edges, and the purple contours represent the target distribution. Finally, 998 unrotated vertices project down to the same bottom-left black point on the plane.

### 4.3 Visualizing the extra-dimensional simplicial sampler

Because of the diminishing returns (Figure 3, right) and  $\mathcal{O}(D^3)$  computational cost associated with increasing the number of simplex vertices, the extra-dimensional simplicial sampler is not practical in the absence of advanced parallelization techniques. Moreover, the rotated vertices no longer maintain equal distances from each other in the low-dimensional space over which the target is defined. Figure 6 shows three successive iterations of the extra-dimensional simplicial sampler with 1000 proposals targeting a 2D Gaussian distribution. The sampler successfully moves to the high-density region of the space in these three steps. We observe that rotating and projection the simplex vertices results in proposal point clouds that look plausibly Gaussian distributed, apparently lacking any geometric structure.

## 5 Discussion

We believe that the simplicial sampler could potentially scale Bayesian inference to extremely high-dimensional problems when implemented on modern graphics processing units (GPU) and successfully combined with other powerful samplers.

Calderhead (2014) demonstrates the natural parallelizability of multiproposal methods. The effective sample size gains reported herein represent an upper bound for efficiency gains that may come with parallelizing the simplicial sampler. We expect the greatest gains will come from (1) implementing the  $\mathcal{O}(D^3)$  matrix multiplications associated with the multiproposal’s random rotation on a GPU and (2) using fine-grained vector processing to evaluate the target density at all proposed states in a way that reduces inter-thread communication associated latency (Holbrook et al., 2021b).

While the multiproposal helps lessen the curse of dimensionality, the simplicial sampler cannot compete with Hamiltonian Monte Carlo (HMC) (Neal, 2011). It may be possible,

however, to combine the two algorithms. Simpl-HMC would (1) rotate a simplex of candidate momenta, (2) simulate Hamiltonian trajectories for each and (3) choose a new state according to canonical density values.

## References

- Andrieu, C., A. Doucet, and R. Holenstein. 2010. Particle markov chain monte carlo methods. *Journal of the Royal Statistical Society: Series B (Statistical Methodology)* 72:269–342.
- Barker, A. A. 1965. Monte carlo calculations of the radial distribution functions for a proton? electron plasma. *Australian Journal of Physics* 18:119–134.
- Borchers, H. W. 2021. *pracma: Practical Numerical Math Functions*. R package version 2.3.3.
- Calderhead, B. 2014. A general construction for parallelizing metropolis- hastings algorithms. *Proceedings of the National Academy of Sciences* 111:17408–17413.
- Delmas, J.-F. and B. Jourdain. 2009. Does waste recycling really improve the multi-proposal metropolis–hastings algorithm? an analysis based on control variates. *Journal of applied probability* 46:938–959.
- Duane, S., A. D. Kennedy, B. J. Pendleton, and D. Roweth. 1987. Hybrid monte carlo. *Physics letters B* 195:216–222.
- Frenkel, D. 2004. Speed-up of monte carlo simulations by sampling of rejected states. *Proceedings of the National Academy of Sciences* 101:17571–17575.
- Gelman, A., W. R. Gilks, and G. O. Roberts. 1997. Weak convergence and optimal scaling of random walk metropolis algorithms. *The annals of applied probability* 7:110–120.
- Green, P. J. 1995. Reversible jump markov chain monte carlo computation and bayesian model determination. *Biometrika* 82:711–732.
- Haario, H., E. Saksman, J. Tamminen, et al. 2001. An adaptive metropolis algorithm. *Bernoulli* 7:223–242.
- Hastings, W. K. 1970. Monte carlo sampling methods using markov chains and their applications .
- Hoffman, M. D. and A. Gelman. 2014. The nouturn sampler: adaptively setting path lengths in hamiltonian monte carlo. *J. Mach. Learn. Res.* 15:1593–1623.
- Holbrook, A. J., X. Ji, and M. A. Suchard. 2020. Bayesian mitigation of spatial coarsening for a fairly flexible spatiotemporal hawkes model. *arXiv preprint arXiv:2010.02994* .
- Holbrook, A. J., X. Ji, and M. A. Suchard. 2021a. From viral evolution to spatial contagion: a biologically modulated hawkes model. *arXiv preprint arXiv:2103.03348* .

- Holbrook, A. J., P. Lemey, G. Baele, S. Dellicour, D. Brockmann, A. Rambaut, and M. A. Suchard. 2021b. Massive parallelization boosts big bayesian multidimensional scaling. *Journal of Computational and Graphical Statistics* 30:11–24.
- Ihaka, R. and R. Gentleman. 1996. R: a language for data analysis and graphics. *Journal of computational and graphical statistics* 5:299–314.
- Lee, J. M. 2012. Quotient Manifolds Pages 540–563. Springer New York, New York, NY.
- Liu, J. S., F. Liang, and W. H. Wong. 2000. The multiple-try method and local optimization in metropolis sampling. *Journal of the American Statistical Association* 95:121–134.
- Metropolis, N., A. W. Rosenbluth, M. N. Rosenbluth, A. H. Teller, and E. Teller. 1953. Equation of state calculations by fast computing machines. *The journal of chemical physics* 21:1087–1092.
- Neal, R. 2011. Mcmc using hamiltonian dynamics. *Handbook of markov chain monte carlo* 2:2.
- Neal, R. M. 2003a. Markov chain sampling for non-linear state space models using embedded hidden markov models. *arXiv preprint math/0305039* .
- Neal, R. M. 2003b. Slice sampling. *Annals of statistics* Pages 705–741.
- Rosenthal, J. S. 2011. Optimal proposal distributions and adaptive mcmc. *Handbook of Markov Chain Monte Carlo* 4.
- Schwedes, T. 2019. Parallel markov chain quasi-monte carlo methods .
- Schwedes, T. and B. Calderhead. 2021. Rao-blackwellised parallel mcmc. Pages 3448–3456 *in* International Conference on Artificial Intelligence and Statistics PMLR.
- Smith, A. F. and G. O. Roberts. 1993. Bayesian computation via the gibbs sampler and related markov chain monte carlo methods. *Journal of the Royal Statistical Society: Series B (Methodological)* 55:3–23.
- Stewart, G. W. 1980. The efficient generation of random orthogonal matrices with an application to condition estimators. *SIAM Journal on Numerical Analysis* 17:403–409.
- Tierney, L. 1994. Markov chains for exploring posterior distributions. *the Annals of Statistics* Pages 1701–1728.
- Tjelmeland, H. 2004. Using all metropolis–hastings proposals to estimate mean values. Tech. rep. Citeseer.
- Williams, C. K. and D. Barber. 1998. Bayesian classification with gaussian processes. *IEEE Transactions on Pattern Analysis and Machine Intelligence* 20:1342–1351.
- Yang, S., Y. Chen, E. Bernton, and J. S. Liu. 2018. On parallelizable markov chain monte carlo algorithms with waste-recycling. *Statistics and Computing* 28:1073–1081.

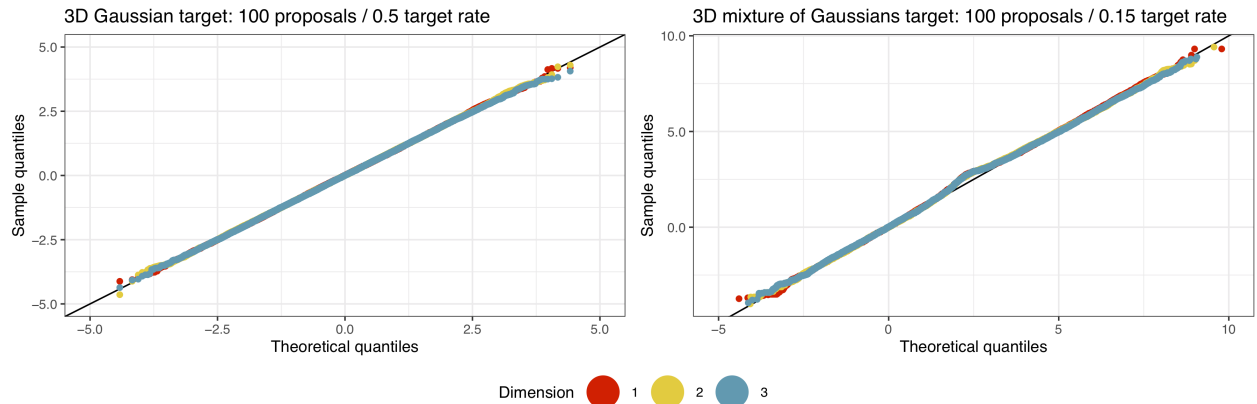


Figure 7: Quantile-quantile plots for the extra-dimensional sampler using a simplex with 101 vertices targeting a 3D Gaussian and mixture of two Gaussian distributions.

Zanella, G. 2020. Informed proposals for local mcmc in discrete spaces. Journal of the American Statistical Association 115:852–865.

## A Empirical accuracy of the extra-dimensional simplicial sampler

We do not prove that the extra-dimensional sampler leaves the target distribution invariant, but limited simulations suggest it might. Figure 7 displays quantile-quantile plots for the sampler using a simplex with 101 vertices and targeting 3D Gaussian and mixture of two Gaussian distributions.